J. Phys. B: At. Mol. Opt. Phys. **31** (1998) 2809–2824. Printed in the UK PII: S0953-4075(98)92011-9

Sum frequency generation from partially ordered media and interfaces: a polarization analysis

David L Andrews and Ian D Hands
School of Chemical Sciences, University of East Anglia, Norwich NR4 7TJ, UK

Received 25 February 1998

Abstract. The theory of sum frequency generation (SFG) is treated within a molecular quantum electrodynamical framework and applied to an ensemble of partially oriented molecules, for lucid analysis of the SFG intensity dependence on beam polarization and molecular symmetry. By expanding the orientational distribution function in terms of an infinite set of Legendre polynomials, it is shown that the observed SFG intensity may be followed in terms of a finite set of distinct contributions. For a time-dependent distribution, each contribution has unique temporal characteristics which may be separated experimentally by manipulation of the laser beam and detection geometry. Specific configurations required for complete separation of the different terms are given. The theory is further developed for partially oriented molecules, within thin films or adsorbed onto surfaces. Consideration is also given to the effect of temperature variation, which should open new avenues for the elucidation of molecular orientation in such media.

1. Introduction

The technique of sum frequency generation (SFG) in optically nonlinear crystals has long been used to produce laser radiation at tailor-made frequencies, but has more recently become an important method of surface analysis. Thus, for example, the mixing of visible and tunable infrared radiation is developing into a powerful spectroscopic method of analysing the vibrations of molecules at, or adsorbed onto, surfaces [1–3]. It is often stated that SFG, like second-harmonic generation (SHG), is surface specific and occurs due to the lack of inversion symmetry necessarily present near an interface [3]. The latter criterion is, however, not an absolute requirement, as witnessed by one of the early SFG experiments in which coherent mixing was achieved within solutions of arabinose [4]. In this paper we present a quantum electrodynamical treatment of SFG for a medium wherein partial molecular order may be apparent. The theory is developed in section 2 and is applicable to molecules oriented in an electric field, and molecules aligned within thin films or adsorbed upon surfaces. Section 3 shows how the orientational averaging may be accomplished and section 4 considers the requirements necessary for observation of the SFG signal. In this section we also discuss some interesting experimental arrangements that could be used to separate the different temporal terms arising from the time-dependent distribution function introduced in section 3. This could be used, for example, to separate the relaxation terms arising due to rotational diffusion. Section 5 looks specifically at ordered molecules within a thin lamina and shows how the concise and general expressions of section 3 may be readily applied to surface studies. Finally, in section 6, we consider the net response of the ensemble to temperature changes and propose experiments for the improved estimation of molecular orientation in surface-oriented layers.

0953-4075/98/122809+16$19.50

2. SFG from oriented molecules

A general expression for the intensity I_{SFG} of SFG from a collection of N molecules may be derived using the standard techniques of quantum electrodynamics [5, 6]. Using the convention that a repeated index implies summation over a complete set of Cartesian coordinates we shall express this intensity in the form:

$$I_{\mathrm{SFG}} = D\left|\bar{e}_i^{(3)} e_j^{(2)} e_k^{(1)} \sum_{\xi}^{N} \beta_{ijk}^{(\xi)} \exp(\mathrm{i}\Delta\boldsymbol{k}\cdot\boldsymbol{R}_\xi)\right|^2, \tag{1}$$

where $\Delta\boldsymbol{k} = \boldsymbol{k}_1 + \boldsymbol{k}_2 - \boldsymbol{k}_3$ is the wavevector mismatch between the input beams (wavevectors $\boldsymbol{k}_1$ and $\boldsymbol{k}_2$) and the emergent radiation at the sum frequency (wavevector $\boldsymbol{k}_3$ and frequency $\omega_3 = \omega_1 + \omega_2$). In equation (1), $\boldsymbol{e}^{(1)}$ and $\boldsymbol{e}^{(2)}$ are the polarization vectors of the input beams and $\boldsymbol{e}^{(3)}$ is the polarization vector for the output (an overbar is used to represent the complex conjugate); $\boldsymbol{R}_\xi$ is the position vector of the molecule ξ and $\beta^{(\xi)}$ is its associated molecular hyperpolarizability tensor defined as:

$$\begin{aligned}\beta_{ijk}^{(\xi)} = \sum_{r,s}\Bigg\{ & \frac{\mu_i^{0s}\mu_j^{sr}\mu_k^{r0}}{(\tilde{E}_{s0} - \hbar\omega_3)(\tilde{E}_{r0} - \hbar\omega_1)} + \frac{\mu_j^{0s}\mu_i^{sr}\mu_k^{r0}}{(\tilde{E}_{s0} + \hbar\omega_2)(\tilde{E}_{r0} - \hbar\omega_1)} \\ & + \frac{\mu_i^{0s}\mu_k^{sr}\mu_j^{r0}}{(\tilde{E}_{s0} - \hbar\omega_3)(\tilde{E}_{r0} - \hbar\omega_2)} + \frac{\mu_k^{0s}\mu_i^{sr}\mu_j^{r0}}{(\tilde{E}_{s0} + \hbar\omega_1)(\tilde{E}_{r0} - \hbar\omega_2)} \\ & + \frac{\mu_j^{0s}\mu_k^{sr}\mu_i^{r0}}{(\tilde{E}_{s0} + \hbar\omega_2)(\tilde{E}_{r0} + \hbar\omega_3)} + \frac{\mu_k^{0s}\mu_j^{sr}\mu_i^{r0}}{(\tilde{E}_{s0} + \hbar\omega_1)(\tilde{E}_{r0} + \hbar\omega_3)}\Bigg\}\end{aligned} \tag{2}$$

where the double sum extends over the complete set of molecular eigenstates and $\mu_l^{ab} = \langle a|\mu_l|b\rangle$ is the lth component of the molecular transition dipole connecting molecular eigenstates $|a\rangle$ and $|b\rangle$. The energy denominators in equation (2) have been written in the complex form $\tilde{E}_{so} = E_s - E_o - \mathrm{i}\Gamma_s$ to account for the damping associated with Γ_s, the linewidth of the excited state $|s\rangle$.

The other factor to define in (1), the beam parameter D, is given by

$$D = \frac{k_3^4 I_{\omega_1} I_{\omega_2}}{32\pi^2 c\varepsilon_0^3}, \tag{3}$$

where I_{ω_i} is the mean irradiance of the input beam of frequency ω_i ($i = 1$ or 2):

$$I_{\omega_i} = \frac{\langle\hat{n}_i\rangle c\hbar\omega_i}{V}, \tag{4}$$

V being the quantization volume and $\langle\hat{n}_i\rangle = \langle\psi(\boldsymbol{k}_i)|\hat{a}^\dagger(\boldsymbol{k}_i)\hat{a}(\boldsymbol{k}_i)|\psi(\boldsymbol{k}_i)\rangle$ the expectation value of the number operator for the general radiation state $|\psi(\boldsymbol{k}_i)\rangle$.

Equation (1) can be written in the equivalent form

$$I_{\mathrm{SFG}} = D\left[\bar{e}_i^{(3)} e_j^{(2)} e_k^{(1)} e_l^{(3)} \bar{e}_m^{(2)} \bar{e}_n^{(1)} \sum_{\xi}^{N}\sum_{\xi'}^{N} \beta_{ijk}^{(\xi)} \bar{\beta}_{lmn}^{(\xi')} \exp(\mathrm{i}\Delta\boldsymbol{k}\cdot\boldsymbol{R}_{\xi\xi'})\right], \tag{5}$$

where $\boldsymbol{R}_{\xi\xi'} = \boldsymbol{R}_\xi - \boldsymbol{R}_{\xi'}$. Thus there are two separable contributions to the SFG:

$$I_{\mathrm{SFG}} = I_{\mathrm{SFG}}^{\mathrm{inc}} + I_{\mathrm{SFG}}^{\mathrm{coh}}, \tag{6}$$

with

$$I_{\mathrm{SFG}}^{\mathrm{inc}} = D\left[\bar{e}_i^{(3)} e_j^{(2)} e_k^{(1)} e_l^{(3)} \bar{e}_m^{(2)} \bar{e}_n^{(1)} \sum_{\xi}^{N} \beta_{ijk}^{(\xi)} \bar{\beta}_{lmn}^{(\xi)}\right] \tag{7}$$

representing the incoherent SFG from individual molecules, and

$$I_{\mathrm{SFG}}^{\mathrm{coh}} = D\left[\bar{e}_i^{(3)} e_j^{(2)} e_k^{(1)} e_l^{(3)} \bar{e}_m^{(2)} \bar{e}_n^{(1)} \sum_{\xi \neq \xi'}^{N} \sum_{\xi'}^{N} \beta_{ijk}^{(\xi)} \bar{\beta}_{lmn}^{(\xi')} \exp(\mathrm{i}\Delta \boldsymbol{k} \cdot \boldsymbol{R}_{\xi\xi'})\right] \tag{8}$$

the coherent SFG associated with interference between signals generated at different molecular centres. In practical terms it is generally this coherent signal with which one is concerned—for perfect phase matching $I_{\mathrm{SFG}}^{\mathrm{coh}}$ has a quadratic dependence on molecular density and hence dominates the much weaker incoherent signal which scales linearly with density. Assuming that the variables describing the orientation of different molecules are independent of one another and that those molecules are constitutionally identical, the orientational average of (8) becomes

$$\begin{aligned} I_{\mathrm{SFG}} \equiv \langle I_{\mathrm{SFG}}^{\mathrm{coh}} \rangle &= D\left[\bar{e}_i^{(3)} e_j^{(2)} e_k^{(1)} e_l^{(3)} \bar{e}_m^{(2)} \bar{e}_n^{(1)} \sum_{\xi \neq \xi'}^{N} \sum_{\xi'}^{N} \langle \beta_{ijk} \rangle \langle \bar{\beta}_{lmn} \rangle \exp(\mathrm{i}\Delta \boldsymbol{k} \cdot \boldsymbol{R})_{\xi\xi'})\right] \\ &= D|\bar{e}_i^{(3)} e_j^{(2)} e_k^{(1)} \langle \beta_{ijk} \rangle|^2 \sum_{\xi \neq \xi'}^{N} \sum_{\xi'}^{N} \exp(\mathrm{i}\Delta \boldsymbol{k} \cdot \boldsymbol{R}_{\xi\xi'}) \end{aligned} \tag{9}$$

where angle brackets have been used to represent an orientational average. Since the result of such an average is necessarily the same for each molecule, the label ξ can be dropped from the β tensor. For generality, we take a weighted orientational average to account for a degree of orientational order within the ensemble—furthermore we allow this degree of ordering to exhibit a time dependence. Incorporating the phase-matching term into the beam parameter by defining:

$$B = D \sum_{\xi \neq \xi'}^{N} \sum_{\xi'}^{N} \exp(\mathrm{i}\Delta \boldsymbol{k} \cdot \boldsymbol{R}_{\xi\xi'}), \tag{10}$$

the expression for the coherent SFG signal is then

$$I_{\mathrm{SFG}} = B|\bar{e}_i^{(3)} e_j^{(2)} e_k^{(1)} \langle \beta_{ijk} \rangle|^2. \tag{11}$$

The theory thus presented in principle applies both to the case of SFG and SHG ($\omega_1 = \omega_2$). However, in the limit where the exact equalities $\boldsymbol{k}_1 = \boldsymbol{k}_2$ and $\boldsymbol{e}^{(1)} = \boldsymbol{e}^{(2)}$ simultaneously hold, the theory at this level of detail reveals a discontinuity of behaviour fundamentally associated with the photon statistics. The problems that this raises, although interesting, are nonetheless peripheral to our present concerns and are therefore to be addressed elsewhere [7]. For the sake of completeness and for use in a later section we shall here simply note that SHG from a single beam can be written in the same form as (11) with

$$B_{\mathrm{SHG}} = \frac{g_\omega^{(2)}}{4} B \tag{12}$$

and with B as given by equation (10), $g_\omega^{(2)}$ being the degree of second-order coherence of the fundamental beam input.

3. Orientational averaging in partially ordered media

To progress further we now need to calculate the orientational average appearing in (11); and this we shall do for a special case—the case where the medium exhibits some partial order.

Let $\hat{\mu}$ be a unit vector in the direction of the molecular alignment axis (normally, though not necessarily, the same direction as the permanent electric dipole moment) and $\hat{\boldsymbol{Z}}$ be a unit vector along the alignment direction of a set of laboratory-fixed axes (X, Y, Z). We shall consider the case of an ensemble of molecules whose orientations may be specified at any time t by a distribution function $f(\theta, t)$, where θ is the angle between the two reference directions $\hat{\mu}$ and $\hat{\boldsymbol{Z}}$, such that $f(\theta, t)\,\mathrm{d}\theta$ is the fractional number of molecules set at an angle between $\theta + \mathrm{d}\theta$. In terms of this distribution function the time-dependent weighted average in equation (11) is given by

$$\langle\beta_{ijk}\rangle = \langle\beta_{ijk} f(\theta, t)\rangle_\Omega / \langle f(\theta, t)\rangle_\Omega. \tag{13}$$

As described in detail in [8], averaging is now accomplished by expanding the distribution function in terms of Legendre polynomials: $f(\theta, t) = \sum_{n=0}^{\infty} a_n(t) P_n\ (\cos\theta)$ where P_n is the Legendre polynomial of order n and $a_n(t)$ is a set of time-dependent coefficients. Thus we require

$$\langle\beta_{ijk}\rangle = \sum_{n=0}^{\infty} a_n(t)\langle\beta_{ijk} P_n(\cos\theta)\rangle_\Omega \Big/ \sum_{n=0}^{\infty} a_n(t)\langle P_n(\cos\theta)\rangle_\Omega. \tag{14}$$

To compute the orientational average over the third rank tensor β we transform into molecular axes, introducing direction cosines of the form $l_{i_r\lambda_r}$, i_r being a component referred to the laboratory fixed frame and λ_r one referred to the molecular frame. Hence we write

$$\langle\beta_{ijk} P_n(\cos\theta)\rangle_\Omega = \beta_{\lambda\mu\nu} I^{(3;n)}_{ijk;\lambda\mu\nu} \tag{15}$$

where

$$I^{(3;n)}_{ijk;\lambda\mu\nu} = \langle l_{i\lambda} l_{j\mu} l_{k\nu} P_n(\cos\theta)\rangle_\Omega. \tag{16}$$

This gives

$$\langle\beta_{ijk}\rangle = \beta_{\lambda\mu\nu} \sum_{n=0}^{\infty} a_n(t) I^{(3;n)}_{ijk;\lambda\mu\nu} \Big/ \sum_{n=0}^{\infty} a_n(t) I^{(0;n)} \tag{17}$$

where the orientational average of the scalar $\langle P_n(\cos\theta)\rangle_\Omega$ has been written as $I^{(0;n)}$ for consistency of notation. Implementation of the requisite orientational averages [9] gives,

$$\langle\beta_{ijk}\rangle = \frac{\beta_{\lambda\mu\nu}}{a_0(t)} \sum_{n=0}^{3} a_n(t) I^{(3;n)}_{ijk;\lambda\mu\nu}. \tag{18}$$

Substitution into (11) then yields

$$I_{\mathrm{SFG}} = B\left|\frac{1}{a_0(t)} \sum_{n=0}^{3} a_n(t) B_n\right|^2 \tag{19}$$

where the coefficients B_n given by

$$B_n = I^{(3;n)}_{ijk;\lambda\mu\nu} \bar{e}^{(3)}_i e^{(2)}_j e^{(1)}_k \beta_{\lambda\mu\nu} \tag{20}$$

carry information on the detailed response, as mediated by the molecular hyperpolarizability, to the polarization field. One immediate consequence of this result is that we can discern a finite number of temporal components contributing to the evolution of SFG from the partially ordered medium. It should be noted that these components are solely associated with the orientational averaging of the hyperpolarizability tensor and not the underlying molecular mechanisms responsible for orientational relaxation. For SHG from molecules reorienting via stochastic rotational diffusion this leads to a signal in the form of a multi-exponential decay as detailed previously [8]. In the general case of SFG, the explicit forms for the coefficients B_n in (20) are

$$B_0 = \tfrac{1}{6}\beta_{\lambda\mu\nu}\varepsilon_{\lambda\mu\nu}(\bar{\boldsymbol{e}}^{(3)} \times \boldsymbol{e}^{(2)}) \cdot \boldsymbol{e}^{(1)} \tag{21}$$

$$B_1 = \frac{1}{30}\begin{bmatrix} (\bar{\boldsymbol{e}}^{(3)} \cdot \boldsymbol{e}^{(2)})(\hat{\boldsymbol{Z}} \cdot \boldsymbol{e}^{(1)}) \\ (\bar{\boldsymbol{e}}^{(3)} \cdot \boldsymbol{e}^{(1)})(\hat{\boldsymbol{Z}} \cdot \boldsymbol{e}^{(2)}) \\ (\boldsymbol{e}^{(2)} \cdot \boldsymbol{e}^{(1)})(\hat{\boldsymbol{Z}} \cdot \bar{\boldsymbol{e}}^{(3)}) \end{bmatrix}^T \begin{bmatrix} 4 & -1 & -1 \\ -1 & 4 & -1 \\ -1 & -1 & 4 \end{bmatrix} \begin{bmatrix} \beta_{\lambda\lambda\mu}\hat{\mu}_\mu \\ \beta_{\lambda\mu\lambda}\hat{\mu}_\mu \\ \beta_{\mu\lambda\lambda}\hat{\mu}_\mu \end{bmatrix} \tag{22}$$

$$\begin{aligned} B_2 = \frac{1}{10} &\begin{bmatrix} (\hat{\boldsymbol{Z}} \cdot \boldsymbol{e}^{(1)})(\bar{\boldsymbol{e}}^{(3)} \times \boldsymbol{e}^{(2)}) \cdot \hat{\boldsymbol{Z}} - \frac{1}{3}(\bar{\boldsymbol{e}}^{(3)} \times \boldsymbol{e}^{(2)}) \cdot \boldsymbol{e}^{(1)} \\ (\hat{\boldsymbol{Z}} \cdot \boldsymbol{e}^{(2)})(\bar{\boldsymbol{e}}^{(3)} \times \boldsymbol{e}^{(1)}) \cdot \hat{\boldsymbol{Z}} + \frac{1}{3}(\bar{\boldsymbol{e}}^{(3)} \times \boldsymbol{e}^{(2)}) \cdot \boldsymbol{e}^{(1)} \end{bmatrix}^T \begin{bmatrix} 2 & -1 \\ -1 & 2 \end{bmatrix} \\ &\times \begin{bmatrix} \beta_{\lambda\mu\nu}\varepsilon_{\lambda\mu\tau}\hat{\mu}_\nu\hat{\mu}_\tau - \frac{1}{3}\beta_{\lambda\mu\nu}\varepsilon_{\lambda\mu\nu} \\ \beta_{\lambda\nu\mu}\varepsilon_{\lambda\mu\tau}\hat{\mu}_\nu\hat{\mu}_\tau + \frac{1}{3}\beta_{\lambda\mu\nu}\varepsilon_{\lambda\mu\nu} \end{bmatrix} \end{aligned} \tag{23}$$

$$\begin{aligned} B_3 = \tfrac{5}{14}[&(\hat{\boldsymbol{Z}} \cdot \bar{\boldsymbol{e}}^{(3)})(\hat{\boldsymbol{Z}} \cdot \boldsymbol{e}^{(2)})(\hat{\boldsymbol{Z}} \cdot \boldsymbol{e}^{(1)}) - \tfrac{1}{5}\{(\bar{\boldsymbol{e}}^{(3)} \cdot \boldsymbol{e}^{(2)})(\hat{\boldsymbol{Z}} \cdot \boldsymbol{e}^{(1)}) \\ &+(\bar{\boldsymbol{e}}^{(3)} \cdot \boldsymbol{e}^{(1)})(\hat{\boldsymbol{Z}} \cdot \boldsymbol{e}^{(2)}) + (\boldsymbol{e}^{(2)} \cdot \boldsymbol{e}^{(1)})(\hat{\boldsymbol{Z}} \cdot \bar{\boldsymbol{e}}^{(3)})\}] \\ &\times[\beta_{\lambda\mu\nu}\hat{\mu}_\lambda\hat{\mu}_\mu\hat{\mu}_\nu - \tfrac{1}{5}\{\beta_{\lambda\lambda\mu}\hat{u}_\mu + \beta_{\lambda\mu\lambda}\hat{\mu}_\mu + \beta_{\mu\lambda\lambda}\hat{\mu}_\mu\}]. \end{aligned} \tag{24}$$

In equation (19) we have a highly compact form for the SFG. One important aspect of the results as expressed above is that they facilitate identification of the circumstances in which individual contributions to the dynamics are manifest. Each of the B_n coefficients may vanish due to experimental configurations, or through constraints on the hyperpolarizability combinations entailed, as we now discuss.

4. Extraction of orientational information and symmetry considerations

The B_0 contribution in equation (19) is necessarily time independent and survives even in the case where (by whatever mechanism) reorientation restores isotropy to a partially ordered medium. This term therefore corresponds to SFG from an ensemble exhibiting bulk isotropy, sustainable only for molecular systems of certain symmetry types (*vide infra*). In the limit as ω_1 approaches ω_2, the hyperpolarizability tensor becomes symmetric in its last two indices so that $\beta_{\lambda\mu\nu}\varepsilon_{\lambda\mu\nu} = 0$; thus SHG is forbidden in isotropic fluid media whereas SFG is not. Equations (19) and (21)–(24) readily allow the polarization characteristics of SFG to be determined through a suitably chosen set of polarization studies, although one must be careful to ensure that any variation in experimental geometry does not introduce a change in the beam parameter B through a concomitant change in phase mismatch. For situations where $\Delta\boldsymbol{k}$ is held constant, polarization studies yield information about the order in the partially oriented medium.

Some interesting and experimentally viable configurations are detailed in figure 1—which indicates that, phase matching notwithstanding, the different temporal contributions are in principle separable. Adopting these geometries, one can readily deduce that the corresponding SFG intensities are given by;

$$I_{\mathrm{SFG}}^{(a)} = \frac{B}{375}\left|\frac{a_1(t)}{a_0(t)}(\beta_{\lambda\lambda\mu} + \beta_{\lambda\mu\lambda} + \beta_{\mu\lambda\lambda})\hat{\mu}_\mu\right|^2, \tag{25a}$$

$$I_{\mathrm{SFG}}^{(b)} = \frac{B}{400}\left|\frac{a_2(t)}{a_0(t)}(\beta_{\lambda\mu\nu} + \beta_{\lambda\nu\mu})\varepsilon_{\lambda\mu\tau}\hat{\mu}_\nu\hat{\mu}_\tau\right|^2 \sin^2 2\beta, \tag{25b}$$

$$I_{\mathrm{SFG}}^{(c)} = \frac{25B}{1568}\left|\frac{a_3(t)}{a_0(t)}[\beta_{\lambda\mu\nu}\hat{\mu}_\lambda\hat{\mu}_\mu\hat{\mu}_\nu - \tfrac{1}{5}(\beta_{\lambda\lambda\mu} + \beta\lambda\mu\lambda + \beta_{\mu\lambda\lambda})\hat{\mu}_\mu]\right|^2, \tag{25c}$$

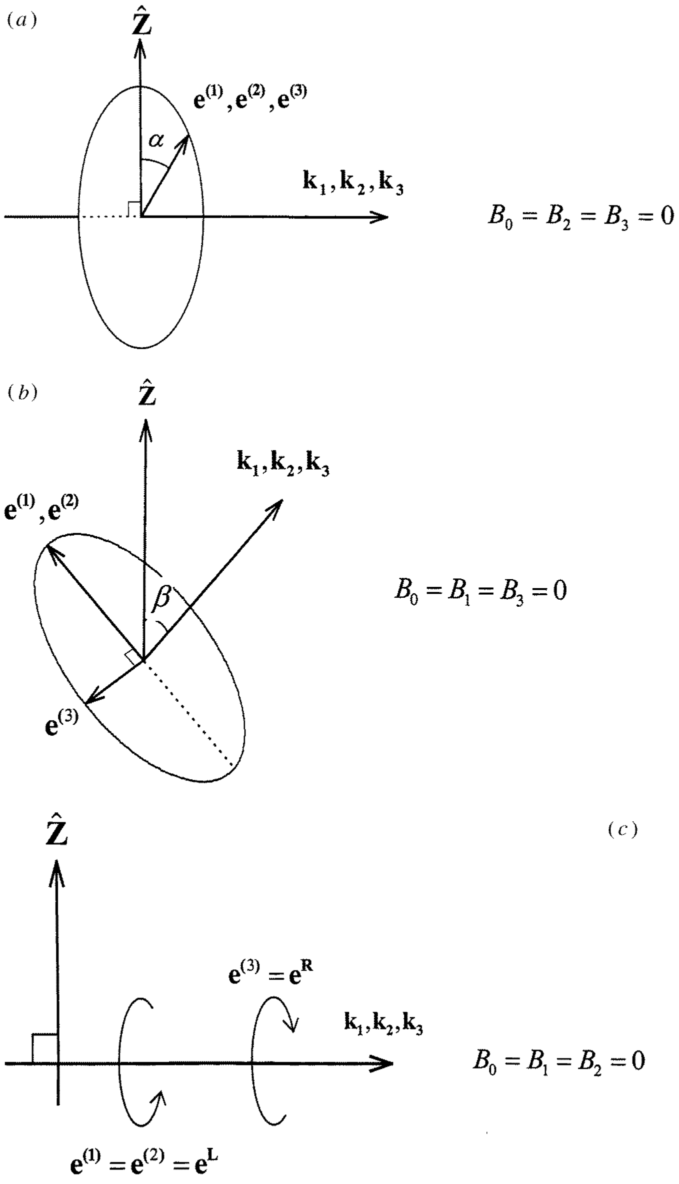

Figure 1. Experimental arrangements for separating the different temporal components contributing to SFG, with $\hat{Z}$ being the direction of preferential alignment. By carefully choosing the wave propagation directions and polarizations we may isolate, in turn, the components depending on the following parameter ratios: (*a*) a_1/a_0; (*b*) a_2/a_0; (*c*) a_3/a_0.

where equation (25*a*) gives the SFG intensity, $I_{\text{SFG}}^{(a)}$, for the arrangement depicted in figure 1(*a*), etc. Some remarks are in order at this point. In case (a) the result given above as equation (25*a*) relates to the specific configuration where $\alpha = 39°14' = \cos^{-1}[(\frac{3}{5})^{1/2}]$; the interest here concerns the fact that B_0, B_2 and B_3 all disappear, leaving a signal governed by the ratio of the a_1 and a_0 temporal coefficients. Similar remarks apply to cases (b) and (c), for which again each result entails the ratio of one other temporal coefficient with

a_0. Thus, monitoring SFG in these situations enables each of the dynamical factors to be separately identified, maximizing the information on the degree of orientational anisotropy in systems aligned by, for example, application of an orienting electric field. Nothing further can be determined, from any form of three-wave mixing, about the other coefficients appearing in the expansion of $f(\theta, t)$. However, if a higher-order nonlinear effect was to be employed then information concerning correspondingly higher-order $a_n(t)$ coefficients would also become available.

Apart from considerations of optical geometry, the coefficients B_n in equations (21)–(24) may completely disappear due to molecular symmetry constraints. Obviously, for molecules possessing inversion symmetry, β is identically zero; for point groups not possessing inversion symmetry the number of independent, non-zero, components may be found using the standard techniques of group theory [10]. Taking the molecular dipole moment to be along the molecular z-axis we can formulate the actual combinations that will be non-zero for the different crystallographic point groups (without the unnecessary assumption of Kleinman index symmetry) [11]—as shown for convenience in table 1. SFG from an isotropic sample ($B_0 \neq 0$) is thus permitted when the molecules in the sample belong to one of the chiral symmetry classes $C_1, C_2, D_2, C_4, D_4, C_3, D_3, C_6, D_6, T$, or O. For partially ordered media, SFG may also arise from the B_1, B_2 and B_3 terms—oriented molecules of C_{2v}, C_{3v}, C_{4v} and C_{6v} symmetry can then be added to the above list of candidates for SFG.

For surface studies, arrangements 1(a) and 1(c) will not be geometrically practicable. The next section considers the problems of phase matching and focuses on surfaces and thin films in order to illustrate the applicability of the theory to this experimentally important case.

5. Application to molecules oriented within thin films and monolayers

The phase-matching double sum

$$S = \sum_{\xi \neq \xi'}^{N} \sum_{\xi'}^{N} \exp(\mathrm{i}\Delta \boldsymbol{k} \cdot \boldsymbol{R}_{\xi\xi'}) \tag{26}$$

featured in equation (10) can be expressed by taking the normal integral limit as

$$S = [N \operatorname{sinc}(\tfrac{1}{2}\Delta k_X A) \operatorname{sinc}(\tfrac{1}{2}\Delta k_Y B) \operatorname{sinc}(\tfrac{1}{2}\Delta k_Z C)]^2 \tag{27}$$

where the N molecules are confined to the region bounded by $0 \leqslant X \leqslant A$, $0 \leqslant Y \leqslant B$ and $0 \leqslant Z \leqslant C$. Clearly, for the partially ordered media to be considered here, the X and Y directions are entirely equivalent. However, we may define a beam geometry whereupon the beams are confined to the (Y, Z)-plane by setting $\Delta k_X = 0$, and also suppose that the sample is a thin film or monolayer in the sense that C is sufficiently small for the approximation $\operatorname{sinc}(\tfrac{1}{2}\Delta k_Z C) \approx 1$ to be valid. Adopting beam arrangements as depicted in figure 2, equation (27) reduces to

$$S = N^2 \operatorname{sinc}^2(\tfrac{1}{2}\Delta k_Y B) \tag{28}$$

with

$$\Delta k_Y = k_1 \sin\theta_1 + k_2 \sin\theta_2 - k_3 \sin\theta_3. \tag{29}$$

The phase-matching condition $\Delta k_Y = 0$ is thus achieved in reflection (and transmission) for angles θ_3 such that

$$\sin\theta_3 = \frac{\omega_1 n(\omega_1) \sin\theta_1 + \omega_2 n(\omega_2) \sin\theta_2}{(\omega_1 + \omega_2) n(\omega_1 + \omega_2)}. \tag{30}$$

Table 1. Non-zero contributions to the hyperpolarizability components in equations (21)–(24).

	$\beta_{\lambda\mu\nu}\varepsilon_{\lambda\mu\nu}$	$\beta_{\lambda\mu z}\varepsilon_{\lambda\mu z}$	$\beta_{\lambda z\mu}\varepsilon_{\lambda\mu z}$	$\beta_{\lambda\lambda z}$	$\beta_{\lambda z\lambda}$	$\beta_{z\lambda\lambda}$	β_{zzz}
C_1	$\beta_{xyz} - \beta_{xzy} + \beta_{zxy} - \beta_{yxz} + \beta_{yzx} - \beta_{zyx}$	$\beta_{xyz} - \beta_{yxz}$	$\beta_{xzy} - \beta_{yzx}$	$\beta_{xxz} + \beta_{yyz} + \beta_{zzz}$	$\beta_{xzx} + \beta_{yzy} + \beta_{zzz}$	$\beta_{zxx} + \beta_{zyy} + \beta_{zzz}$	β_{zzz}
C_2	$\beta_{xyz} - \beta_{xzy} + \beta_{zxy} - \beta_{yxz} + \beta_{yzx} - \beta_{zyx}$	$\beta_{xyz} - \beta_{yxz}$	$\beta_{xzy} - \beta_{yzx}$	$\beta_{xxz} + \beta_{yyz} + \beta_{zzz}$	$\beta_{xzx} + \beta_{yzy} + \beta_{zzz}$	$\beta_{zxx} + \beta_{zyy} + \beta_{zzz}$	β_{zzz}
C_{2v}	0	0	0	$\beta_{xxz} + \beta_{yyz} + \beta_{zzz}$	$\beta_{xzx} + \beta_{yzy} + \beta_{zzz}$	$\beta_{zxx} + \beta_{zyy} + \beta_{zzz}$	β_{zzz}
D_2	$\beta_{xyz} - \beta_{xzy} + \beta_{zxy} - \beta_{yxz} + \beta_{yzx} - \beta_{zyx}$	$\beta_{xyz} - \beta_{yxz}$	$\beta_{xzy} - \beta_{yzx}$	0	0	0	0
C_4	$2(\beta_{xyz} - \beta_{xzy} + \beta_{zxy})$	$2\beta_{xyz}$	$2\beta_{xzy}$	$2\beta_{xxz} + \beta_{zzz}$	$2\beta_{xzx} + \beta_{zzz}$	$2\beta_{zxx} + \beta_{zzz}$	β_{zzz}
C_{4v}	0	0	0	$2\beta_{xxz} + \beta_{zzz}$	$2\beta_{xzx} + \beta_{zzz}$	$2\beta_{zxx} + \beta_{zzz}$	β_{zzz}
D_4	$2(\beta_{xyz} - \beta_{xzy} + \beta_{zxy})$	$2\beta_{xyz}$	$2\beta_{xzy}$	0	0	0	0
C_3	$2(\beta_{xyz} - \beta_{xzy} + \beta_{zxy})$	$2\beta_{xyz}$	$2\beta_{xzy}$	$2\beta_{xxz} + \beta_{zzz}$	$2\beta_{xzx} + \beta_{zzz}$	$2\beta_{zxx} + \beta_{zzz}$	β_{zzz}
C_{3v}	0	0	0	$2\beta_{xxz} + \beta_{zzz}$	$2\beta_{xzx} + \beta_{zzz}$	$2\beta_{zxx} + \beta_{zzz}$	β_{zzz}
D_3	$2(\beta_{xyz} - \beta_{xzy} + \beta_{zxy})$	$2\beta_{xyz}$	$2\beta_{xzy}$	0	0	0	0
C_6	$2(\beta_{xyz} - \beta_{xzy} + \beta_{zxy})$	$2\beta_{xyz}$	$2\beta_{xzy}$	$2\beta_{xxz} + \beta_{zzz}$	$2\beta_{xzx} + \beta_{zzz}$	$2\beta_{zxx} + \beta_{zzz}$	β_{zzz}
C_{6v}	0	0	0	$2\beta_{xxz} + \beta_{zzz}$	$2\beta_{xzx} + \beta_{zzz}$	$2\beta_{zxx} + \beta_{zzz}$	β_{zzz}
D_6	$2(\beta_{xyz} - \beta_{xzy} + \beta_{zxy})$	$2\beta_{xyz}$	$2\beta_{xzy}$	0	0	0	0
T	$3(\beta_{xyz} - \beta_{xzy})$	$\beta_{xyz} - \beta_{xzy}$	$-(\beta_{xyz} - \beta_{xzy})$	0	0	0	0
O	$6\beta_{xyz}$	$2\beta_{xyz}$	$-\beta_{xyz}$	0	0	0	0

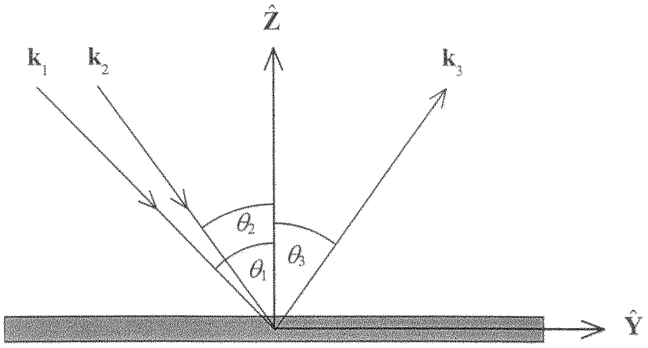

Figure 2. Wave geometries for surface and thin film studies in reflection (and for $\theta_3 > \pi/2$ transmission). The $\hat{\boldsymbol{X}}$-direction is out of the plane towards the reader.

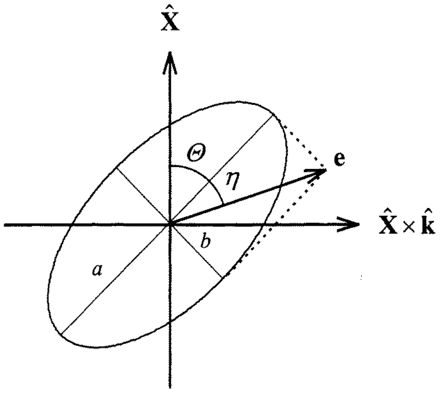

Figure 3. Convention used for light with elliptical polarization. The beam is travelling outwards from the paper with wavevector $\boldsymbol{k}$; the azimuth Θ is the angle between the major axis of the ellipse and the laboratory-fixed $\hat{\boldsymbol{X}}$ axis in the sense shown, and $\eta = \tan^{-1}(b/a)$ is the ellipticity, where a is the length of the major axis and b is that of the minor axis.

Assuming the SFG signal is detected in the phase-matched direction, we now consider various possibilities with regards to polarization analysis. As indicated by equation (28), the phase-matched geometry implies that $S = N^2$. As the angles of incidence, θ_1 and θ_2, of the incoming beams are varied the number of molecules exposed to both beams will vary. For two input beams of identical circular section centred on the same point on the surface we find that

$$S = \rho_{\mathrm{s}}^2 A^2 \sec^2 \theta_{\min} \tag{31}$$

where ρ_{s} is the surface density of molecules in the thin film, A is the cross sectional area of the incoming beams and $\theta_{\min} = \min(\theta_1, \theta_2)$ is the smaller of the two angles of incidence, which dictates the common area of beam overlap at the surface.

To account for all experimental possibilities we shall allow each of the three beams under consideration to assume a generalized state of elliptical polarization. This entails defining two parameters: the ellipticity η and azimuth Θ, as defined in figure 3 following the convention of Hecht and Barron [12]. To keep the expressions for SFG intensities as compact as possible, however, it is better to define the polarizations in terms of three parameters (σ, ϕ, ζ) which in turn relate to the usual definitions. To this end we define:

$$\begin{aligned} \boldsymbol{e}^{(1)} &= \mathrm{e}^{\mathrm{i}\phi_1} \cos\sigma_1 \hat{\boldsymbol{X}} + \mathrm{e}^{\mathrm{i}\zeta_1} \sin\sigma_1 \hat{\boldsymbol{X}} \times \hat{\boldsymbol{k}}_1 \\ \boldsymbol{e}^{(2)} &= \mathrm{e}^{\mathrm{i}\phi_2} \cos\sigma_2 \hat{\boldsymbol{X}} + \mathrm{e}^{\mathrm{i}\zeta_2} \sin\sigma_2 \hat{\boldsymbol{X}} \times \hat{\boldsymbol{k}}_2 \\ \boldsymbol{e}^{(3)} &= \mathrm{e}^{\mathrm{i}\phi_3} \cos\sigma_3 \hat{\boldsymbol{X}} + \mathrm{e}^{\mathrm{i}\zeta_3} \sin\sigma_3 \hat{\boldsymbol{X}} \times \hat{\boldsymbol{k}}_3 \end{aligned} \tag{32}$$

where, for each beam, (σ, ϕ, ζ) relate to the azimuth and ellipticity as defined in figure 3 through:

$$\mathrm{e}^{\mathrm{i}\sigma} = \frac{(1+\cos 2\Theta \cos 2\eta)^{1/2} + \mathrm{i}(1-\cos 2\Theta\cos 2\eta)^{1/2}}{\sqrt{2}} \tag{33}$$

$$\mathrm{e}^{\mathrm{i}\phi} = \frac{1-\mathrm{i}\tan\Theta\tan\eta}{(1+\tan^2\Theta\tan^2\eta)^{1/2}} \tag{34}$$

$$\mathrm{e}^{\mathrm{i}\zeta} = \frac{\tan\Theta + \mathrm{i}\tan\eta}{(\tan^2\Theta + \tan^2\eta)^{1/2}}. \tag{35}$$

Using these relations we can deduce the required mappings for commonly used experimental geometries:

$$(\sigma,\phi,\zeta) \mapsto \begin{cases} (\pi/4, 0, \pi/2) & \text{R-circularly polarized light } (\Theta = 0, \eta = \pi/4) \\ (\pi/4, 0, -\pi/2) & \text{L-circularly polarized light } (\Theta = 0, \eta = -\pi/4) \\ (\pi/2, 0, 0) & \text{p-linearly polarized light } (\Theta = \pi/2, \eta = 0) \\ (0,0,0) & \text{s-linearly polarized light } (\Theta = 0, \eta = 0). \end{cases} \tag{36}$$

Returning to the SFG intensity, we can now express the B_n coefficients in the following matrix form:

$$B_0 = \tfrac{1}{6}\tilde{B}_0\beta_{\lambda\mu\nu}\varepsilon_{\lambda\mu\nu} \tag{37}$$

$$B_1 = \tfrac{1}{30}\tilde{\boldsymbol{B}}_1^T \begin{bmatrix} 4 & -1 & -1 \\ -1 & 4 & -1 \\ -1 & -1 & 4 \end{bmatrix} \begin{bmatrix} \beta_{\lambda\lambda\mu}\hat{\mu}_\mu \\ \beta_{\lambda\mu\lambda}\hat{\mu}_\mu \\ \beta_{\mu\lambda\lambda}\hat{\mu}_\mu \end{bmatrix} \tag{38}$$

$$B_2 = \tfrac{1}{10}\tilde{\boldsymbol{B}}_2^T \begin{bmatrix} 2 & -1 \\ -1 & 2 \end{bmatrix} \begin{bmatrix} \beta_{\lambda\mu\nu}\varepsilon_{\lambda\mu\tau}\hat{\mu}_\nu\hat{\mu}_\tau - \tfrac{1}{3}\beta_{\lambda\mu\nu}\varepsilon_{\lambda\mu\nu} \\ \beta_{\lambda\nu\mu}\varepsilon_{\lambda\mu\tau}\hat{\mu}_\nu\hat{\mu}_\tau + \tfrac{1}{3}\beta_{\lambda\mu\nu}\varepsilon_{\lambda\mu\nu} \end{bmatrix} \tag{39}$$

$$B_3 = \tfrac{5}{14}\tilde{B}_3[\beta_{\lambda\mu\nu}\hat{\mu}_\lambda\hat{\mu}_\mu\hat{\mu}_\nu - \tfrac{1}{5}(\beta_{\lambda\lambda\mu} + \beta_{\lambda\mu\lambda} + \beta_{\mu\lambda\lambda})\hat{\mu}_\mu] \tag{40}$$

and using (32) gives:

$$\begin{aligned} \tilde{B}_0 = {} & \mathrm{e}^{\mathrm{i}(\zeta_1+\zeta_2-\phi_3)}\sin\sigma_1\sin\sigma_2\cos\sigma_3\sin(\theta_1-\theta_2) + \mathrm{e}^{\mathrm{i}(\zeta_1+\phi_2-\zeta_3)}\sin\sigma_1\cos\sigma_2\sin\sigma_3\sin(\theta_1+\theta_3) \\ & -\mathrm{e}^{\mathrm{i}(\phi_1+\zeta_2-\zeta_3)}\cos\sigma_1\sin\sigma_2\sin\sigma_3\sin(\theta_2+\theta_3) \end{aligned} \tag{41}$$

$$\tilde{\boldsymbol{B}}_1 = \begin{bmatrix} \mathrm{e}^{\mathrm{i}\zeta_1}\sin\theta_1\sin\sigma_1(\mathrm{e}^{\mathrm{i}(\phi_2-\phi_3)}\cos\sigma_2\cos\sigma_3 - \mathrm{e}^{\mathrm{i}(\zeta_2-\zeta_3)}\sin\sigma_2\sin\sigma_3\cos(\theta_2+\theta_3)) \\ \mathrm{e}^{\mathrm{i}\zeta_2}\sin\theta_2\sin\sigma_2(\mathrm{e}^{\mathrm{i}(\phi_1-\phi_3)}\cos\sigma_1\cos\sigma_3 - \mathrm{e}^{\mathrm{i}(\zeta_1-\zeta_3)}\sin\sigma_1\sin\sigma_3\cos(\theta_1+\theta_3)) \\ \mathrm{e}^{\mathrm{i}\zeta_3}\sin\theta_3\sin\sigma_3(\mathrm{e}^{\mathrm{i}(\phi_1+\phi_2)}\cos\sigma_1\cos\sigma_2 + \mathrm{e}^{\mathrm{i}(\zeta_1+\zeta_2)}\sin\sigma_1\sin\sigma_2\cos(\theta_1-\theta_2)) \end{bmatrix} \tag{42}$$

$$\tilde{\boldsymbol{B}}_2 = \begin{bmatrix} \mathrm{e}^{\mathrm{i}\zeta_1}\sin\theta_1\sin\sigma_1(\mathrm{e}^{\mathrm{i}(\zeta_2-\phi_3)}\cos\theta_2\sin\sigma_2\cos\sigma_3 + \mathrm{e}^{\mathrm{i}(\phi_2-\zeta_3)}\cos\theta_3\cos\sigma_2\sin\sigma_3) - \tilde{B}_0/3 \\ \mathrm{e}^{\mathrm{i}\zeta_2}\sin\theta_2\sin\sigma_2(\mathrm{e}^{\mathrm{i}(\zeta_1-\phi_3)}\cos\theta_1\sin\sigma_1\cos\sigma_3 + \mathrm{e}^{\mathrm{i}(\phi_1-\zeta_3)}\cos\theta_3\cos\sigma_1\sin\sigma_3) + \tilde{B}_0/3 \end{bmatrix} \tag{43}$$

$$\begin{aligned} \tilde{B}_3 = {} & \mathrm{e}^{\mathrm{i}(\zeta_1+\zeta_2-\zeta_3)}\sin\theta_1\sin\theta_2\sin\theta_3\sin\sigma_1\sin\sigma_2\sin\sigma_3 \\ & -\tfrac{1}{5}\{\mathrm{e}^{\mathrm{i}\zeta_1}\sin\theta_1\sin\sigma_1(\mathrm{e}^{\mathrm{i}(\phi_2-\phi_3)}\cos\sigma_2\cos\sigma_3 - \mathrm{e}^{\mathrm{i}(\zeta_2-\zeta_3)}\sin\sigma_2\sin\sigma_3\cos(\theta_2+\theta_3)) \\ & +\mathrm{e}^{\mathrm{i}\zeta_2}\sin\theta_2\sin\sigma_2(\mathrm{e}^{\mathrm{i}(\phi_1-\phi_3)}\cos\sigma_1\cos\sigma_3 - \mathrm{e}^{\mathrm{i}(\zeta_1-\zeta_3)}\sin\sigma_1\sin\sigma_3\cos(\theta_1+\theta_3)) \\ & +\mathrm{e}^{\mathrm{i}\zeta_3}\sin\theta_3\sin\sigma_3(\mathrm{e}^{\mathrm{i}(\phi_1+\phi_2)}\cos\sigma_1\cos\sigma_2 + \mathrm{e}^{\mathrm{i}(\zeta_1+\zeta_2)}\sin\sigma_1\sin\sigma_2\cos(\theta_1-\theta_2))\}. \end{aligned} \tag{44}$$

It is important to check, *inter alia*, that the expressions thus derived reduce to previously established results for the case of SHG. Assuming that phase matching occurs at an angle $\theta_3 = \theta_1 = \theta_2 = \theta$, and setting $(\sigma_1, \phi_1, \zeta_1) = (\sigma_2, \phi_2, \zeta_2) = (\sigma, \phi, \zeta)$ for the fundamental beam with $\omega = \omega_1 = \omega_2$, and $(\sigma_3, \phi_3, \zeta_3) = (\sigma', \phi', \zeta')$ for the second-harmonic beam at 2ω, equations (41)–(44) reduce to

$$\tilde{B}_0 = 0 \tag{45}$$

$$\tilde{\boldsymbol{B}}_1 = \sin\theta \begin{bmatrix} e^{i\zeta} \sin\sigma\,(e^{i(\phi-\phi')} \cos\sigma \cos\sigma' - e^{i(\zeta-\zeta')} \sin\sigma \sin\sigma' \cos 2\theta) \\ e^{i\zeta} \sin\sigma\,(e^{i(\phi-\phi')} \cos\sigma \cos\sigma' - e^{i(\zeta-\zeta')} \sin\sigma \sin\sigma' \cos 2\theta) \\ e^{i\zeta'} \sin\sigma'(e^{2i\phi} \cos^2\sigma + e^{2i\zeta} \sin^2\sigma) \end{bmatrix} \tag{46}$$

$$\tilde{\boldsymbol{B}}_2 = e^{i\zeta} \sin\theta \cos\theta \sin\sigma\,(e^{i(\zeta-\phi')} \sin\sigma \cos\sigma' + e^{i(\phi-\zeta')} \cos\sigma \sin\sigma') \begin{bmatrix} 1 \\ 1 \end{bmatrix} \tag{47}$$

$$\begin{aligned} \tilde{B}_3 = {} & e^{i(2\zeta-\zeta')} \sin^3\theta \sin^2\sigma \sin\sigma' \\ & -\frac{\sin\theta}{5}\{2e^{i\zeta} \sin\sigma\,(e^{i(\phi-\phi')} \cos\sigma \cos\sigma' - e^{i(\zeta-\zeta')} \sin\sigma \sin\sigma' \cos 2\theta) \\ & +e^{-i\zeta'} \sin\sigma\,(e^{2i\phi} \cos^2\sigma + e^{2i\zeta} \sin^2\sigma)\}. \end{aligned} \tag{48}$$

Two important special cases can now be readily treated.

5.1. SHG with plane polarized input

With linearly polarized input the polarization plane of the reflected harmonic is in general rotated with respect to the polarization plane of the incoming fundamental. Here we must set $\phi = \phi' = \zeta = \zeta' = 0$ which, using equations (3), (10), (12), (19), (31), (37)–(40) and (46)–(48) yields,

$$I_{\mathrm{SHG}} = \frac{g_\omega^{(2)} k_{2\omega}^4 I_\omega^2 \rho_s^2 A^2}{128\pi^2 c\varepsilon_0^3} \sec^2\theta \left| \frac{a_1}{a_0} B_1 + \frac{a_2}{a_0} B_2 + \frac{a_3}{a_0} B_3 \right|^2 \tag{49}$$

where

$$\begin{aligned} B_1 = {} & \frac{\sin\theta}{30}\{(3\beta_{\lambda\lambda\mu} + 3\beta_{\lambda\mu\lambda} - 2\beta_{\mu\lambda\lambda}) \sin\sigma \cos\sigma \cos\sigma' - (\beta_{\lambda\lambda\mu} + \beta_{\lambda\mu\lambda} - 4\beta_{\mu\lambda\lambda}) \sin\sigma' \\ & -(3\beta_{\lambda\lambda\mu} + 3\beta_{\lambda\mu\lambda} - 2\beta_{\mu\lambda\lambda}) \sin^2\sigma \sin\sigma' \cos 2\theta\}\hat{\mu}_\mu \end{aligned} \tag{50}$$

$$B_2 = \frac{\sin\theta\cos\theta}{10} \sin\sigma \sin(\sigma + \sigma')(\beta_{\lambda\mu\nu} + \beta_{\lambda\nu\mu})\varepsilon_{\lambda\mu\tau}\hat{\mu}_\nu\hat{\mu}_\tau \tag{51}$$

$$\begin{aligned} B_3 = {} & \frac{5\sin\theta}{14}[\sin^2\theta \sin^2\sigma \sin\sigma' - \tfrac{1}{5}\{2\sin\sigma\,(\cos\sigma \cos\sigma' - \sin\sigma \sin\sigma' \cos 2\theta) + \sin\sigma'\}] \\ & \times[\beta_{\lambda\mu\nu}\hat{\mu}_\lambda\hat{\mu}_\mu\hat{\mu}_\nu - \tfrac{1}{5}(\beta_{\lambda\lambda\mu} + \beta_{\lambda\mu\lambda} + \beta_{\mu\lambda\lambda})\hat{\mu}_\mu]. \end{aligned} \tag{52}$$

These expressions are quite general. Using $I_{\mathrm{p/s}}^{\mathrm{p/s}}$ to denote the second-harmonic intensities obtained when the fundamental (superscript) and second harmonic (subscript) have p- or s-polarization we obtain:

$$I_{\mathrm{p}}^{\mathrm{p}} = \frac{g_\omega^{(2)} k_{2\omega}^4 I_\omega^2 \rho_s^2 A^2}{128\pi^2 c\varepsilon_0^3} \tan^2\theta |C_1 \sin^2\theta + C_2 \cos^2\theta|^2 \tag{53}$$

$$I_{\mathrm{s}}^{\mathrm{p}} = \frac{g_\omega^{(2)} k_{2\omega}^4 I_\omega^2 \rho_s^2 A^2}{128\pi^2 c\varepsilon_0^3} \sin^2\theta |C_3|^2 \tag{54}$$

$$I_{\mathrm{p}}^{\mathrm{s}} = \frac{g_\omega^{(2)} k_{2\omega}^4 I_\omega^2 \rho_s^2 A^2}{128\pi^2 c\varepsilon_0^3} \tan^2\theta |C_4|^2 \tag{55}$$

$$I_{\mathrm{s}}^{\mathrm{s}} = 0 \tag{56}$$

with the (complex) constants C_1–C_4 given by

$$C_1 = \frac{a_1}{15a_0}(\beta_{\lambda\lambda\mu} + \beta_{\lambda\mu\lambda} + \beta_{\mu\lambda\lambda})\hat{\mu}_\mu + \frac{a_3}{7a_0}(\beta_{\lambda\mu\nu}\hat{\mu}_\lambda\hat{\mu}_\mu\hat{\mu}_\nu - \tfrac{1}{5}(\beta_{\lambda\lambda\mu} + \beta_{\lambda\mu\lambda} + \beta_{\mu\lambda\lambda})\hat{\mu}_\mu) \tag{57}$$

$$C_2 = \frac{-a_1}{15a_0}(2\beta_{\lambda\lambda\mu} + 2\beta_{\lambda\mu\lambda} - 3\beta_{\mu\lambda\lambda})\hat{\mu}_\mu + \frac{a_3}{14a_0}(\beta_{\lambda\mu\nu}\hat{\mu}_\lambda\hat{\mu}_\mu\hat{\mu}_\nu - \tfrac{1}{5}(\beta_{\lambda\lambda\mu} + \beta_{\lambda\mu\lambda} + \beta_{\mu\lambda\lambda})\hat{\mu}_\mu) \tag{58}$$

$$C_3 = \frac{a_2}{10a_0}(\beta_{\lambda\mu\nu} + \beta_{\lambda\nu\mu})\varepsilon_{\lambda\mu\tau}\hat{\mu}_\nu\hat{\mu}_\tau \tag{59}$$

$$C_4 = \frac{a_1}{30a_0}(\beta_{\lambda\lambda\mu} + \beta_{\lambda\mu\lambda} - 4\beta_{\mu\lambda\lambda})\hat{\mu}_\mu + \frac{a_3}{14a_0}(\beta_{\lambda\mu\nu}\hat{\mu}_\lambda\hat{\mu}_\mu\hat{\mu}_\nu - \tfrac{1}{5}(\beta_{\lambda\lambda\mu} + \beta_{\lambda\mu\lambda} + \beta_{\mu\lambda\lambda})\hat{\mu}_\mu). \tag{60}$$

The dependence of the second-harmonic intensities on the angle of incidence indicated in equations (53)–(56) is identical to that derived by Byers *et al* [13] and Hecht and Barron [12]. Equation (54) indicates, as mentioned in [13], that the occurrence of s-polarized SHG from a p-polarized fundamental beam is a ready indication of surface chirality—the coefficient C_3, as is apparent from table 1, being non-zero only for chiral species. The treatment here however additionally gives the explicit dependence on the preferred orientation of the molecules present in the thin film via the orientational parameters a_n. One would expect these parameters to be highly temperature dependent, and so one can confidently predict that the combination of temperature programming and polarization analysis will yield a wealth of valuable new information on orientation at surfaces.

5.2. SHG with circularly polarized input

The second important case concerns the circular intensity difference (CID) between the SHG intensities produced by circularly polarized light of difference handedness. Setting $(\sigma, \phi, \zeta) = (\pi/4, 0, \pm\pi/2)$, where the upper sign refers to R-polarized light, and considering linearly polarized output so that $\phi' = \zeta' = 0$, the expression for the second-harmonic intensity has the form given by (49) with

$$B_1 = \frac{\sin\theta}{60}(\pm\mathrm{i}\cos\sigma' + \sin\sigma'\cos 2\theta)(3\beta_{\lambda\lambda\mu} + 3\beta_{\lambda\mu\lambda} - 2\beta_{\mu\lambda\lambda})\hat{\mu}_\mu \tag{61}$$

$$B_2 = \frac{\sin\theta\cos\theta}{20}(-\cos\sigma' \pm \mathrm{i}\sin\sigma')(\beta_{\lambda\mu\nu} + \beta_{\lambda\nu\mu})\varepsilon_{\lambda\mu\tau}\hat{\mu}_\nu\hat{\mu}_\tau \tag{62}$$

$$\begin{aligned} B_3 = \frac{-5\sin\theta}{14}&[\tfrac{1}{2}\sin^2\theta\sin\sigma' + \tfrac{1}{5}(\pm\mathrm{i}\cos\sigma' + \sin\sigma'\cos 2\theta)] \\ &\times[\beta_{\lambda\mu\nu}\hat{\mu}_\lambda\hat{\mu}_\mu\hat{\mu}_\nu - \tfrac{1}{5}(\beta_{\lambda\lambda\mu} + \beta_{\lambda\mu\lambda} + \beta_{\mu\lambda\lambda})\hat{\mu}_\mu]. \end{aligned} \tag{63}$$

For the detection of p-polarized light we have, using obvious notation:

$$I_{\mathrm{p}}^{\mathrm{R}} = \frac{g_\omega^{(2)}k_{2\omega}^4 I_\omega^2 \rho_{\mathrm{s}}^2 A^2}{512\pi^2 c\varepsilon_0^3}\tan^2\theta|(C_1 + C_4)\sin^2\theta + (C_2 + C_4)\cos^2\theta - \mathrm{i}C_3\cos\theta|^2 \tag{64}$$

$$I_{\mathrm{p}}^{\mathrm{L}} = \frac{g_\omega^{(2)}k_{2\omega}^4 I_\omega^2 \rho_{\mathrm{s}}^2 A^2}{512\pi^2 c\varepsilon_0^3}\tan^2\theta|(C_1 + C_4)\sin^2\theta + (C_2 + C_4)\cos^2\theta + \mathrm{i}C_3\cos\theta|^2 \tag{65}$$

and for s-polarized SHG:

$$I_{\mathrm{s}}^{\mathrm{R}} = \frac{g_\omega^{(2)}k_{2\omega}^4 I_\omega^2 \rho_{\mathrm{s}}^2 A^2}{512\pi^2 c\varepsilon_0^3}\tan^2\theta|(C_2 + C_4) - \mathrm{i}C_3\cos\theta|^2 \tag{66}$$

$$I_{\mathrm{s}}^{\mathrm{L}} = \frac{g_{\omega}^{(2)} k_{2\omega}^{4} I_{\omega}^{2} \rho_{\mathrm{s}}^{2} A^{2}}{512\pi^{2} c \varepsilon_{0}^{3}} \tan^{2}\theta |(C_{2} + C_{4}) + \mathrm{i}C_{3}\cos\theta|^{2} \tag{67}$$

with the C_n coefficients as given by equations (57)–(60). Again, the dependence of equations (64)–(67) on the angle of incidence θ is seen to match previous results from Byers *et al* [14] and Hecht and Barron [12]. The equations readily show that CIDs ($I_{\mathrm{s}}^{\mathrm{R}} \neq I_{\mathrm{s}}^{\mathrm{L}}, I_{\mathrm{p}}^{\mathrm{R}} \neq I_{\mathrm{p}}^{\mathrm{L}}$) occur only: (i) for chiral substances and (ii) where the molecular hyperpolarizability contains an appreciable imaginary component. The latter condition, as is apparent from equation (2), dictates that we are near to resonance.

Although studies of wavelength dependence have been performed [13–16], SHG remains a purely electronic technique, and we expect that the chiral effects discussed above will become even more important and useful when combined with visible-tunable IR SFG where vibrational resonances may be exploited. Expressions (41)–(44), and the SFG expressions ensuing therefrom, will therefore be of value in deciphering the profusion of information likely to follow from such experiments.

6. Temperature-dependent SFG studies

As a specific example of the use of the more general SFG expressions given here we consider the problem of determining the orientation of molecules adsorbed onto surfaces or interfaces. As already mentioned, this information is embodied within the coefficients a_n appearing in the Legendre polynomial expansion of the orientational distribution function. Thus we need to find ways to determine as much information as possible about the individual a_n terms. In general the SFG and SHG intensity will depend on several of these coefficients simultaneously. However, SFG has the advantage over SHG that there are a greater number of independently variable parameters at the disposal of the experimentalist. For the case of visible-tunable IR SFG experiments there is, of course, the additional benefit that vibrational resonances may be used to enhance the SFG signal.

Letting ω_1 be the visible frequency, ω_2 be the IR frequency and ω_3 be the sum frequency we can take advantage of the fact that phase matching will occur when $\theta_3 \approx \theta_1$, to simplify the SFG intensity expressions. Two interesting experimental configurations may then be found from equations (41)–(44).

(i) When $\theta_2 = 0$ and a ppp configuration is adopted (where the polarizations are given in the order $\omega_1\omega_2\omega_3 = \omega_{\mathrm{vis}}\omega_{\mathrm{IR}}\omega_{\mathrm{SFG}}$), the SFG intensity,

$$I_{\mathrm{SFG}}^{(1)} \propto (a_1/a_0)^2. \tag{68}$$

(ii) When $\theta_2 = \theta_3 = \theta_1 \neq 0$ and a pps configuration is adopted, the SFG intensity,

$$I_{\mathrm{SFG}}^{(2)} \propto (a_2/a_0)^2. \tag{69}$$

If the temperature of the thin film is varied, the SFG intensity will vary and the variation will be different for the two different arrangements outlined above. The intensities given in (68) and (69) are moderated by many factors and so the absolute values of the intensities will not in general be directly useful. However, the variation in SFG with temperature will be primarily due to the change in molecular orientation and so the gradient of the SFG intensity versus T plots will contain useful orientational information. Indeed, temperature-dependent SFG studies of this general kind have only recently been used to study the phase transition within monolayers of 1-undecanol upon a surface of D_2O [17].

Here, as a simple example, consider molecules adsorbed onto a surface such that their preferred direction of orientation is at an angle θ_0 to the surface. Let us further suppose that the molecules are distributed normally about their preferred orientation direction so that the orientational distribution function takes the form

$$f(\theta) = \exp\{-c(\theta - \theta_0)^2/T\}. \tag{70}$$

In (70), T is the absolute temperature and c is a characteristic orientational temperature, a constant measuring how firmly the molecules are restrained towards their preferred orientation. For this distribution we find

$$\frac{a_1}{a_0} = \frac{3S_2(c,T)}{2S_1(c,T)} \tag{71}$$

and

$$\frac{a_2}{a_0} = \frac{5}{8}\left(\frac{3S_3(c,T)}{S_1(c,T)} - 1\right) \tag{72}$$

where we have defined the integral function

$$S_n(c,T) = \int_0^{\pi} \sin n\theta \exp\{-c(\theta-\theta_0)^2/T\}\,\mathrm{d}\theta. \tag{73}$$

We now define two dimensionless ratios related to the fractional changes with temperatures of the SFG intensity, for the cases considered above:

$$R_1 \equiv \frac{T}{I_{\mathrm{SFG}}^{(1)}}\frac{\partial I_{\mathrm{SFG}}^{(1)}}{\partial T} = \frac{2c}{T}\left(\frac{S_2'}{S_2} - \frac{S_1'}{S_1}\right) \tag{74}$$

and

$$R_2 \equiv \frac{T}{I_{\mathrm{SFG}}^{(2)}}\frac{\partial I_{\mathrm{SFG}}^{(2)}}{\partial T} = \frac{6c}{T}\left(\frac{S_3'}{S_3} - \frac{S_1'}{S_1}\right)\left(3 - \frac{S_1}{S_3}\right)^{-1} \tag{75}$$

where

$$S_n'(c,T) = \int_0^{\pi} (\theta-\theta_0)^2 \sin n\theta \exp\{-c(\theta-\theta_0)^2/T\}\,\mathrm{d}\theta. \tag{76}$$

It is apparent from (73)–(76) that R_1 and R_2 depend only on θ_0 and the ratio $r = T/c$. Figure 4 shows the variation of R_1 and R_2, for several values of θ_0, over a wide range of r values. For $\theta_0 = 0, r = 0.01$ corresponds to a 'tight' distribution of orientations such that the distribution function f falls to half of its maximum value after $\sim 5^\circ$; $r = 0.7$ corresponds to a 'loose' distribution where f drops to its half maximum at $\sim 40^\circ$. By performing the temperature variation experiments described above we can measure the ratios R_1 and R_2 at a particular temperature and use the graphs in figure 4 to determine values for r and θ_0. As the temperature is known, we can hence deduce values for c and θ_0. Such experiments will allow critical evaluation of the functions used to model the orientational distribution of molecules on surfaces and lead to a deeper understanding of adsorption itself.

7. Conclusion

We have shown that a quantum electrodynamical treatment of sum frequency generation leads to very compact expressions for the SFG intensity. The relations are, furthermore, easy to interpret for any given configuration of laser beam directions and polarizations.

Although use of SFG as a spectroscopic technique for the identification of vibrational resonances is well known, we have shown that in several other aspects SFG offers advantages over SHG as a tool for the study of partially ordered media and surfaces. A simple example has been given to illustrate that reliable information about orientation and distribution of

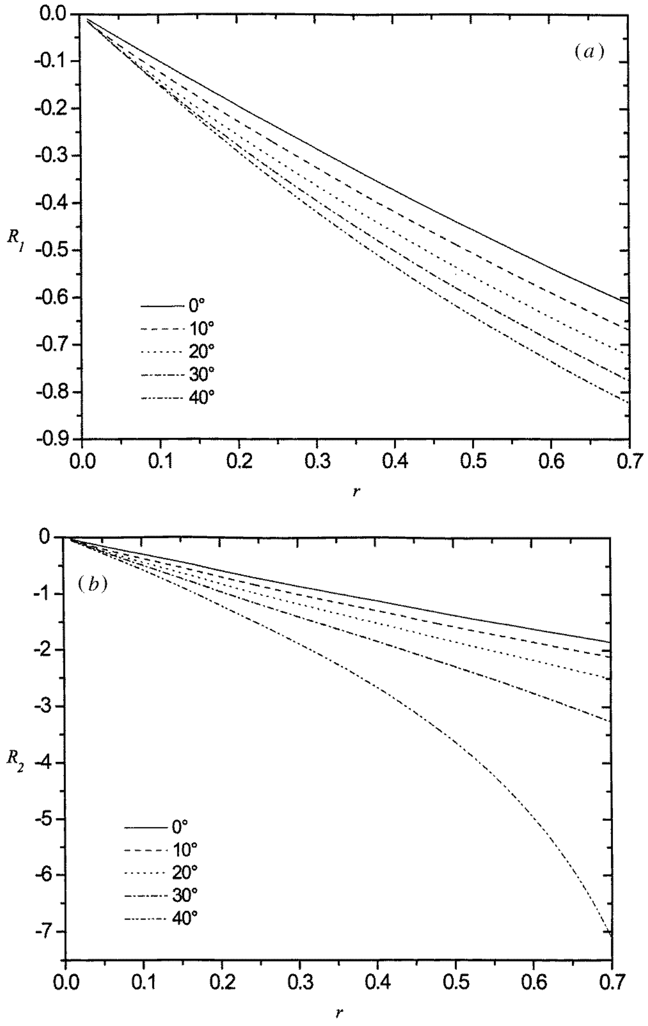

Figure 4. Graphs showing the ratios (*a*) R_1 and (*b*) R_2 for five preferred orientation angles, $\theta_0 = 0°$, $20°$, $30°$ and $40°$ over a large range of the dimensionless parameter $r = T/c$.

molecules within thin films or adsorbed onto surfaces may be available by temperature-programmed SFG studies.

Finally, although SHG occurs only from the surface of fluid media exhibiting bulk isotropy, the same is not generally true for SFG. Indeed it is surprising that the technique of SFG is not routinely used to monitor reactions involving the loss or creation of chiral species—an obvious application of the earliest demonstration of the effect [4]. Based on the theory presented here, such a method should, perhaps, be considered as a useful tool for such investigations in future experiments.

Acknowledgments

Funding for this work from the Engineering and Physical Sciences Research Council is gratefully acknowledged and we also thank Dr S R Meech for helpful comments on the manuscript.

References

[1] Eisenthal K B 1996 *Chem. Rev.* **96** 1343
[2] Bell G R, Bain C D and Ward R N 1996 *J. Chem. Soc. Faraday Trans.* **92** 515
[3] Shen Y R 1996 *Proc. Natl. Acad. Sci., USA* **93** 12 104
[4] Rentzepis P M, Giordmaine J A and Wecht K W 1966 *Phys. Rev. Lett.* **16** 792
[5] Craig D P and Thirunamachandran T 1984 *Molecular Quantum Electrodynamics* (London: Academic)
[6] Andrews D L 1993 *Advan. Chem. Phys. (Modern Nonlinear Optics 2)* vol 85, ed M Evans and S Kielich p 545
[7] Andrews D L and Hands I D Work in progress
[8] Andrews D L and Hands I D 1996 *Chem. Phys.* **213** 277
[9] Andrews D L and Harlow M J 1984 *Phys. Rev.* A **29** 2796
[10] Bhagavantam S and Suryanarayana D 1949 *Acta Cryst.* **2** 21
[11] Barron L D 1982 *Molecular Light Scattering and Optical Activity* (Cambridge: Cambridge University Press)
[12] Hecht L and Barron L D 1996 *Mol. Phys.* **89** 61
[13] Byers J D, Yee H I and Hicks J M 1994 *J. Chem. Phys.* **101** 6233
[14] Byers J D, Yee H I, Petralli-Mallow T and Hicks J M 1994 *Phys. Rev.* B **49** 14 643
[15] Heinz T F, Chen C K, Ricard D and Shen Y R 1982 *Phys. Rev. Lett.* **48** 478
[16] Crawford M J, Haslam S, Probert J M, Gruzdkov Y A and Frey J G 1994 *Chem. Phys. Lett.* **229** 260
[17] Braun R, Casson B D and Bain C D 1995 *Chem. Phys. Lett.* **245** 326